GEOTECHNICAL EXTREME EVENTS RECONNAISSANCE (GEER) ASSOCIATION

Turning Disaster into Knowledge

THE KFARNABRAKH LANDSLIDE OF NOVEMBER 30TH, 2015:
A Geological and Geotechnical Evaluation of the Landslide and Risk of Future Failures

Report of the NSF Sponsored GEER Association Team

Authors:

Chadi S. El Mohtar
Associate Professor, University of Texas at Austin, Austin, Texas

Grace Abou-Jaoude
Assistant Professor, Lebanese American University, Byblos, Lebanon

Chadi Abdallah
Senior Researcher, Lebanese National Council for Scientific Research, Beirut, Lebanon

Jacques Harb
Notre Dame University-Louaize, Zouk Mosbeh, Lebanon

GEER Association Report No. GEER-047

March 16, 2016

THE KFARNABRAKH LANDSLIDE OF NOVEMBER 30TH, 2015:
A Geological and Geotechnical Evaluation of the Landslide and Risk of Future Failures

Authors:

Chadi S. El Mohtar
Associate Professor, University of Texas at Austin, Austin, Texas

Grace Abou-Jaoude
Assistant Professor, Lebanese American University, Byblos, Lebanon

Chadi Abdallah
Senior Researcher, Lebanese National Council for Scientific Research, Beirut, Lebanon

Jacques Harb
Notre Dame University-Louaize, Zouk Mosbeh, Lebanon

Acknowledgements:

The authors would like to extend thanks to the researchers of the Remote Sensing Center at the Lebanese National Council for Scientific Research (CNRS-L) for their technical assistance in GIS mapping and 3D modelling, particularly, Mr. Fadi KassHanna and Mr. Hussein Khatib (early field investigations), Mr. Ali Kumaiha (acquired drone photos), and Mr. Bashar Mekdad and Ms. Samah Termos (photo processing). We also thank Dr. Ihab Jomaa from the Lebanese Agriculture Research Institute and Mr. Rachid Jomaa from the Center of Geophysics, CNRS-L for providing respectively the rainfall and seismic activity data for the region. This report wouldn't be possible without the geological expertise of Mr. Abed Hajj Chehadeh, a Research Assistant at the Lebanese American University, Byblos, Lebanon. Last but not least, a special thanks goes to the local residents of the town of Kfarnabrakh for being very welcoming and providing their detailed recollection of the relevant history of the area, particularly Mr. Dorayd Houssam-ElDeen who walked us through the area and provided valuable information. Thanks extended to the CNRS authority for being part in funding this research.

The work of the GEER Association, in general, is based upon work supported in part by the National Science Foundation through the Geotechnical Engineering Program under Grant No. CMMI-1266418. Any opinions, findings, and conclusions or recommendations expressed in this

material are those of the authors and do not necessarily reflect the views of the NSF. The GEER Association is made possible by the vision and support of the NSF Geotechnical Engineering Program Directors: Dr. Richard Fragaszy and the late Dr. Cliff Astill. GEER members also donate their time, talent, and resources to collect time-sensitive field observations of the effects of extreme events.

Introduction

During the early hours of November 30th, 2015, the mountain town of Kfarnabrakh experienced a major landslide at one of the town's rock cliffs. Kfarnabrakh is 1,150 meters above the sea level, 45 km south-east of Beirut, and about 30 km away from the Mediterranean seacoast (Figure 1). The rock cliffs are located at the north-northeast edge of the village with houses constructed within few meters of the cliff edges (33°42'01"N 35°37'42"E). Seventeen houses were evacuated and the families were provided monetary compensation to secure temporary housing until the stability and safety of the sliding zone is assessed.

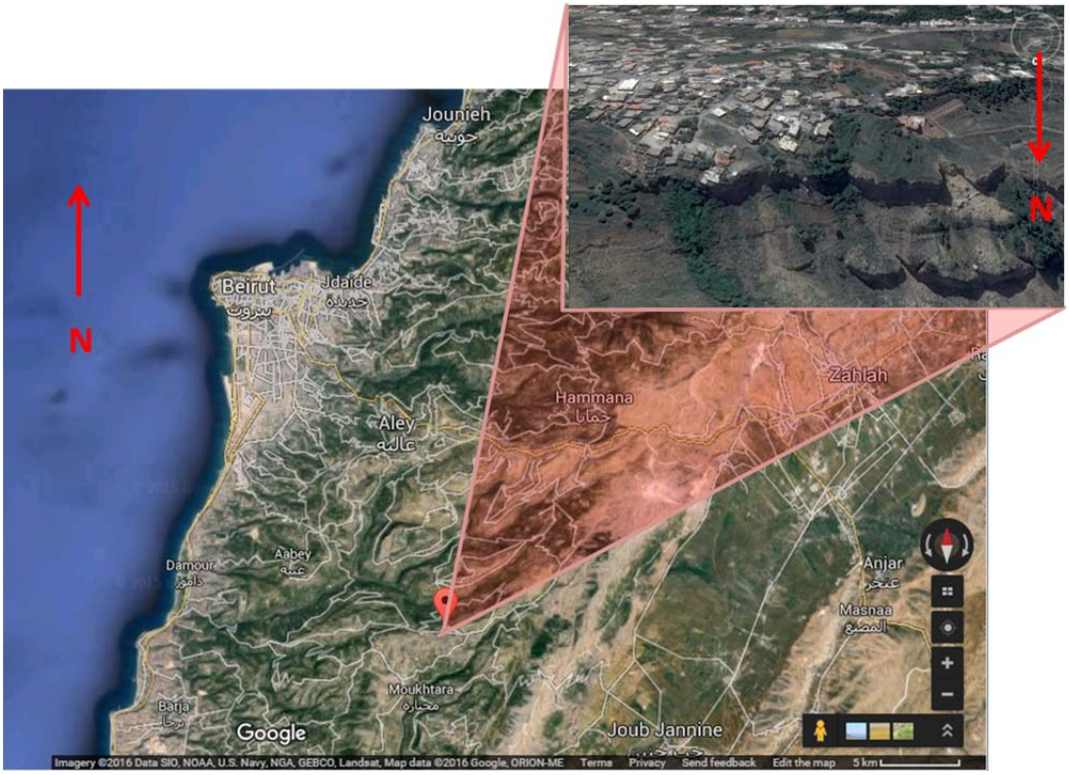

Figure 1: Location of the landslide (Pictures from Google Earth Pro)

- **History of failures in the area**

The area is known to have witnessed historical landslides that are deep seated and can be easily identified in the field. Particularly, local poets and historians recollect a major landslide on January 18th, 1767 which resulted in major losses of property, a number of deaths (exact record not available), and dislocation of farm lands along the north-west slopes of the town. This landslide, as identified from current field topography (Figure 2), resulted in the current steep cliffs where the 2015 landslide occurred. More recent, the area experienced a landslide in 2012, about a 100m away (center to center) from the 2015 landslide. Figure 3 shows a view of the cliff with both landslides identified. Also shown in the figure is a retaining wall that was constructed following the 2012 landslide to protect the road and farm land at the base of the cliff from debris

flow. It is worth mentioning here that several small faults exist in the area (see Figure 6 in the following section), although most of these are not active.

Figure 2: Interpreted field image of the historical 1767 Kfarnabrakh Landslide (picture take at 33°42'22"N 35°37'25"E).

Figure 3: Location of the 2012 and 2015 landslides (Picture generated form Point cloud 3D representation)

- **Site visits and locals recollection of the failure**

The 2015 landslide was well documented with cellphone videos captured by the local residents. One of these videos is posted at the following link and will be later used in analyzing the failure mechanism: (https://www.youtube.com/watch?v=1qTtrICtT-A&feature=youtu.be).

The GEER team conducted multiple site visits and collected some of the local residents' recollections of the failure. Below are some of the points brought up:

- Cracking in the rocks with three very loud cracking sounds. Failure accompanied by shaking.
- The failure took around 45 minutes but most of the videos capture the last 2-5 minutes
- Rocks exploding and shooting out of the blue marl layer (although this is more likely to be parts of the blue marl rather than actual rocks as will be discussed later).
- The presence of a cave beneath the built houses.
- The failed block rotated rather than slid (this is not consistent with what was scene in the videos).
- No significant rain prior to the failure.
- It happens every 4th year during leap year.

Below are some additional observations by the GEER team from the site visits:

- The top soil has a very low hydraulic conductivity and there is a local "spring" that residents described as a year round spring with no seasonal change in water supply (Appendix Figure A.1).
- The rock mass is highly jointed with joint spacing of less than 1m even in the top portion of the cliff that appeared as a massive rock (Appendix Figure A.2 and 3).
- There are new cracks that started to form at a new location between the 2012 and 2015 failures which is a clear indication of possible near future failures (Appendix Figure A.4).
- There is evidence of water stream at the base of the cliff with running water observed during our site visit (Appendix Figure A.5).
- A large number of houses have been evacuated and the damage from the latest landslide started reaching the backyards of these houses (Appendix Figure A.6).
- The retaining wall constructed following the 2012 landslide was able to block the debris during the Nov. 2015 landslide; however, it did sustain punctures and detachment damage from rolling stones as can be seen in Figure 4 after the first site visit. The wall backside was filled up with detriments showing a lack of maintenance. That explains why the damage occurred on the upper part of the wall.
- The retaining wall didn't fare well in terms of protecting the road on January 3rd, 2016 after having 116 mm of rainfall over 3 days (Figure 5). The fresh debris from the November landslide were mobilized again and caused complete closure of the road adjacent to the retaining wall. The inspected stones were ranging from weak and poor weathered limestones to very stiff dolomitic stones. For reference, the elevation change between the top of the cliff and the base of the wall is about 250 m.

Figure 4: Damage to the Retaining wall following Nov. 2015 landslide (Picture taken at from 33°42’13”N 35°37’36”E)

Figure 5: Overtopping of wall due to debris flow following heavy rainfall in January 3rd, 2016 (Picture taken at 33°42’10”N 35°37’33”E)

Local Geology

The Kfarnabrakh area consists mainly of pseudo-tabular lower Cretaceous rocks. These are incised by the westward flowing Safa River. An entire stratigraphic sequence can be observed on the northern flank of this drainage facing Kfarnabrakh as shown in Figure 6. A cross-section of the formations near the failure area along line AB is presented in Figure 7. The stratigraphy is superimposed over the cliff surface image in Figure 8 to show the alignment of the different strata with the outcrop.

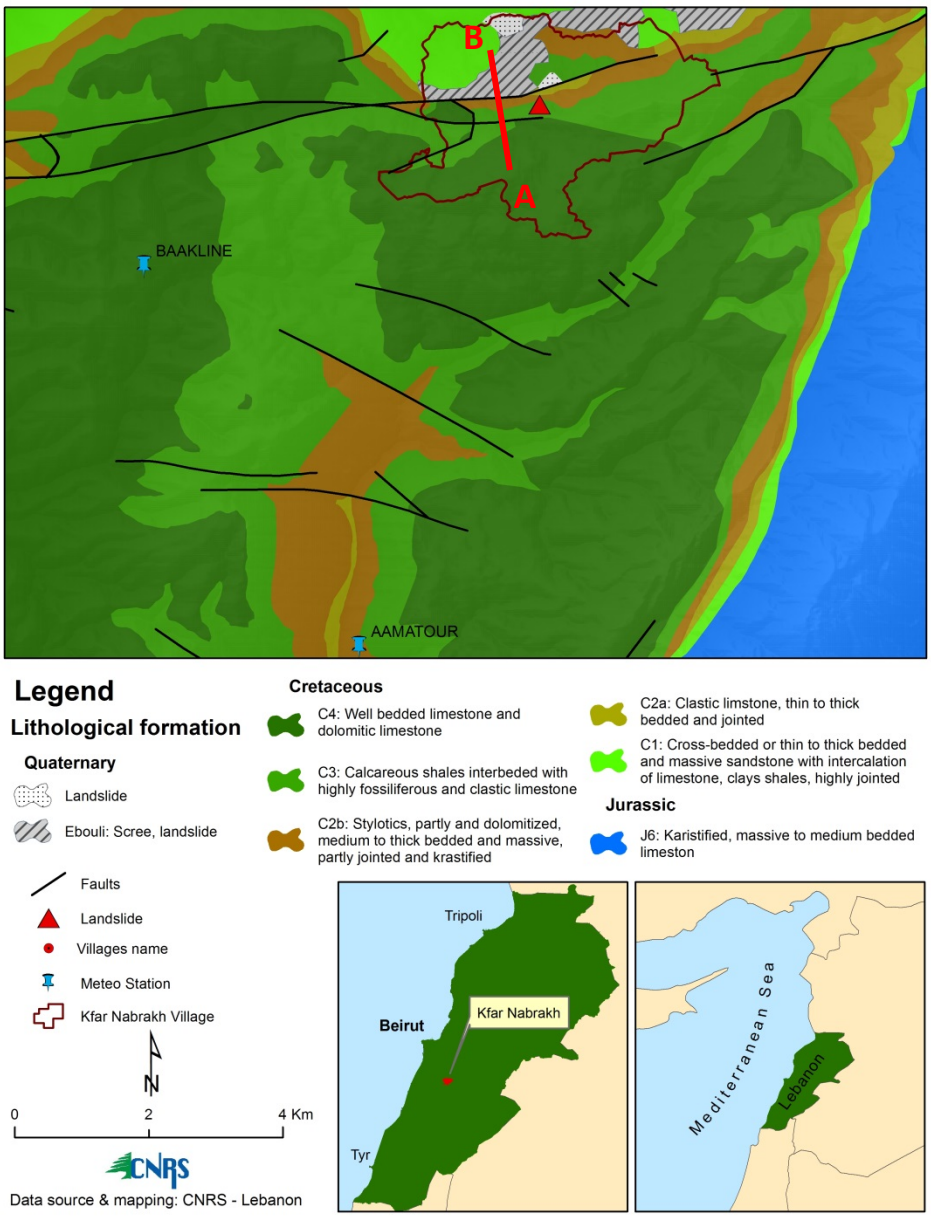

Figure 6: Geologic Map of the Kfarnabrakh area.

This rock sequence is subdivided into five rock formations and ranked according to their stratigraphic ages from oldest to youngest by Dubertret (1945), Walley (1983) and Walley (1997). The formations are:

C1 Formation:

The C1, also known as the Chouf formation consists of beige to white colored sandstone sometimes rich in Iron oxide. It is composed of fine to coarse grained quartz sands and sandstones, intercalated with horizons of clay, coal, lignite. Its early sedimentary units locally host a volcanic member consisting of basalts and volcanic tuff.

C2a Formation:

The C2a, also known as the Abeih formation, consists of ochre yellow to brown rock units. Its gastropod and bivalve rich stratum consists of terrigenous and marine detrital material, It is a moderately thick-bedded, clastic limestone, interbedded with marly argillaceous sandy limestones and shales.

C2b Formation:

The C2b, also known as the Mdeirej formation (*muraille blanche*), it consists generally of a massive, thick bedded, jointed, stylolitic, partially karstified limestone and dolomitic limestone and can be stratigraphically separated into two units of two

- The lower unit is a 50-60m thick, pale grey and cliff forming rock unit composed of micritic limestone.
- The upper unit is made of marly limestone layers that reaches 55m in thickness.

C3 Formation:

The C3, also known as the Hammana Formation, consists of an approximately 120m of thin-bedded, marly limestone and shales, upgrading into moderately thick-bedded limestone, interbedded with marl The rocks composing this formation are usually highly friable and poor conductors of water. This reflects their low shear strength and low permeability. **The 2015 failure zone is stratigraphically located in the mid C3 formation as indicated on Figures 7 and 8 below.**

C4 Formation:

The C4, also known as the Sannine formation, is the most dominant formation in Lebanon (40%). It is formed of chert-bearing, massive to thinly bedded, highly fractured and jointed outcrops. It is a well karstified limestone and dolomitic limestone.

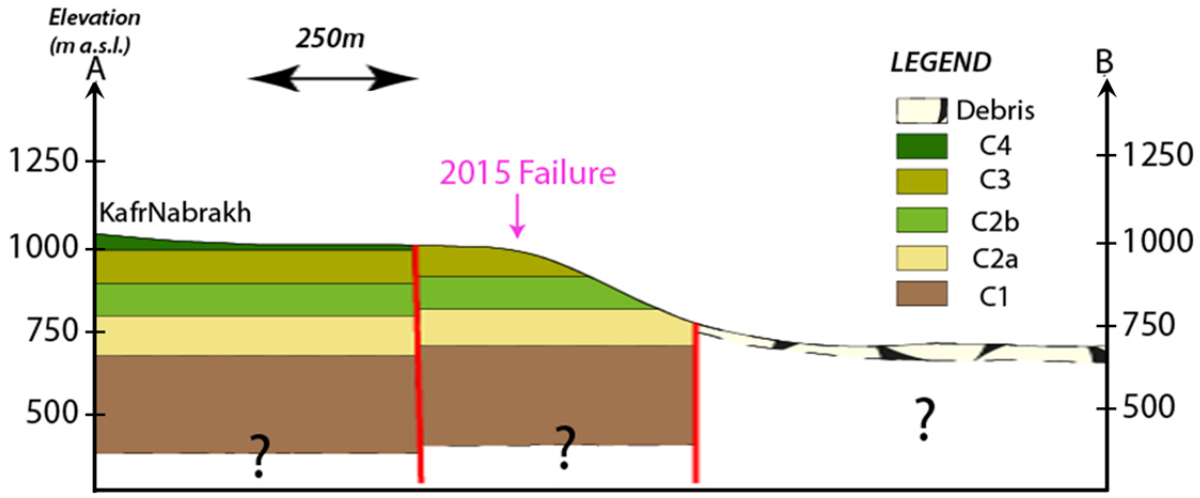

Figure 7: Geologic cross section along line AB from Figure 6

Figure 8: Interpreted pan view showing a detailed stratigraphy of the Kfarnabrakh failure zone (Picture generated form Point cloud 3D representation)

Local Hydrogeology

Figure 9 shows the local hydrogeology with the different basins and surface flow channels. The location of the landslide (presented by the red triangle on the map) indicates that the cliffs fall in the Aptian-Albian (C2-C3) unproductive basins. However, there is the Jezzine Cretaceous Basin on the southeast side and Metn-Chouf Sandstone basin on the north east of it. These 2 basins can provide a water source for flow through the highly jointed C2 formation in which the failure has occurred. This scenario explains the presence of water springs at the top and bottom of the cliff, even though it falls in a non-productive formation. It also explains the high density of wells in the area.

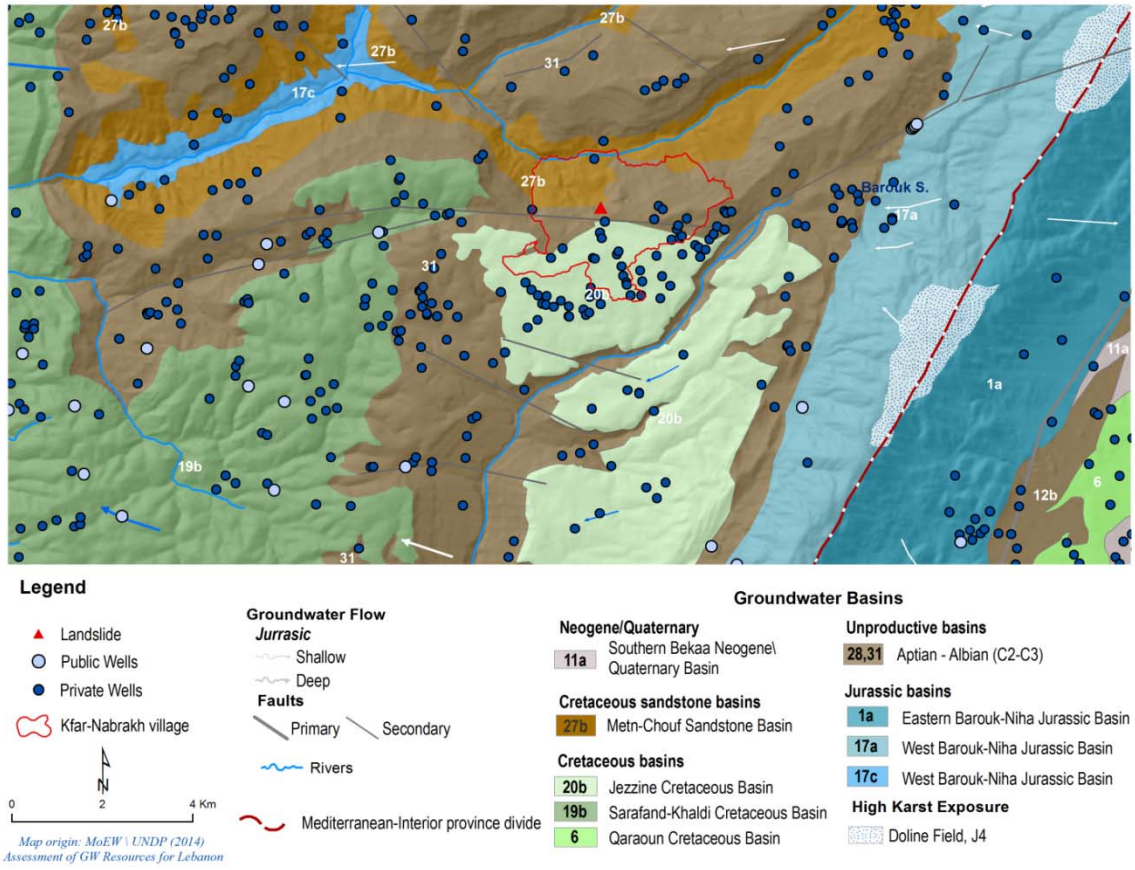

Figure 9: Hydrogeologic map of the surrounding region

Mapping the 2015 Landslide

- **Aerial Photography acquisition and Digital Surface Model (DSM) Generation**

The surveying flight for Kfarnabrakh was carried out on the 25th of December 2015. The area of the slide and its surrounding was recorded in 11 East–West strips (Figure 9). A GoPro camera with a focal length of 30 mm was used and the total surface area covered was around 0.652 km^2 (65.2 Hectare). This surface area was covered by 363 aerial photographs with a long-track

overlaps at 60% and across-track at 30% and an average ground sampling distance (GSD) of 5.32 cm. During the aerial photo acquisition the traveling speed of the carrier was 11m/s and the altitude exceeded 100m above the launching site (on the cliff beside the slide). The details of the aerial photo acquisition are presented in Table 1.

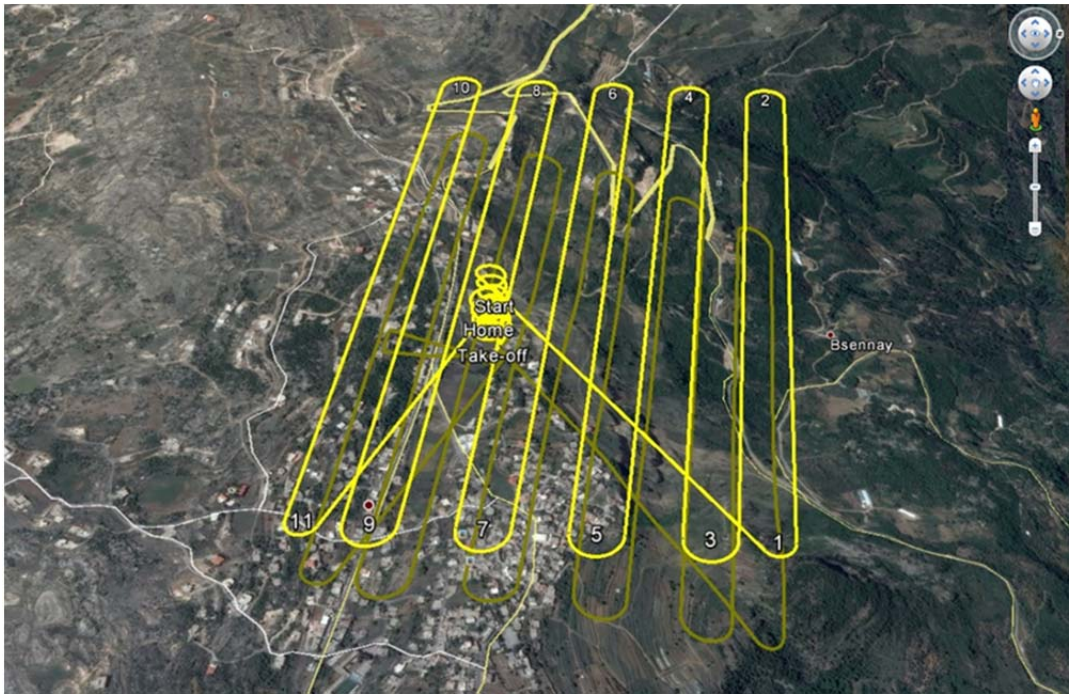

Figure 10: Drone Flight path (From Google Earth Pro)

Table 1: Details of the aerial photo acquisition

Area covered	0.652 Km^2
Camera name	GoPro
Sensor size	6.24
Focal length	30 mm
Image coordinate system	Double stereographic of Lebanon datum: Levant
Flight path	11 E-W
Average ground sampling distance	5.32 cm
Number of images	363
DEM resolution	10 cm
Matching quality	Median of 13507 matches per calibrated image
Georeferencing	4 GCPs

After the aerial photo acquisition and before performing any image analysis, the camera data were geometrically rectified (Geo-referenced) with respect to a map projection system. The geo-referencing was carried out with the available GCPs. For further use, this data was transformed into the national object coordinate system Double stereographic projection of Lebanon by applying regional transformation parameters. The Georeferencing operation concerns the sensor

orientation and includes the determination of the exterior orientation along the flight trajectory of each of the 11 flight strips and the resampling of the scanner data into the object coordinate system. With the help of some control points, the GPS model was shifted and rotated to correct the datum definition. Each block (set of images in each strip) was considered as an image pair. After collecting the Tie points and the GCPs, four steps were taken for generating the DSM: 1) epipolar image creation, 2) image matching, 3) DSM geocoding and 4) gap filling and mosaicking.

First the Epipolar Image generation was created. The epipolar geometry describes the geometrical constraint between two frame images of a stereo pair (here identified as the Blocks). It represents the fact that a ground point and the two optical centers lie on the same plane. This means that for a given point in one image, its conjugate point in the other image must lie on a known line in the second image. By creating epipolar images, the search space for finding corresponding image points in automatic image matching is reduced. The image matching finds the conjugate points on both the left and right images which correspond to the same ground feature. The output of the image matching procedure is called a parallax image, in which the x-coordinate difference (along epipolar lines) between the left and right image is stored and is used to build the DSM. After that, the six DSMs were geocoded and re-projected from the epipolar projection to the output map projection (Double stereo) and units of meters. All six strips were then mosaicked and the failed and/or incorrect values were filled and resampled to the pixel spacing. **The resultant was a DSM of 10 cm resolution**.

Finally, in order to benefit from the 3D stereo capability of the aerial photo acquisition, both the orthorectified blocks of the image and the produced DSM were synchronized into the same extent and resolution so that they can be combined into 4 raster bands R, G, B, Z. The results are shown below in Figure 11.

Figure 11: Point cloud 3D representation for Kfarnabrakh landslides

Local Conditions Prior to Landslide

- **Seismic data**

With reference to the CNRS Geophysical Center seismic station, there were no records of any seismic activity beyond ambient noise at the time of the failure.

- **Rainfall data**

Rainfall data were collected from two stations located closest to Kfarnabrakh. The Amatour station is located 5.6 km south of Kfarnabrakh and about 160m lower in elevation above sea level; the Baakline station is about 6 km south west of Kfarnabrakh and 175m lower in elevation. The location of the 2 stations relative to the area of the failure is included in Figure 6. Figure 12 shows the accumulation of rainfall starting October 1st, 2015 through January 9th, 2016. The rainfall data was collected every 2 hours at both stations. The records confirm the local residents' recollection that there was no major rainfall in the days leading to the landslide on November 30th. The records also show over 110mm of precipitation in the 3 days leading to the January 3rd, 2016 debris flow that lead to overtopping of the protection wall and complete closure of the road at the toe of the cliff.

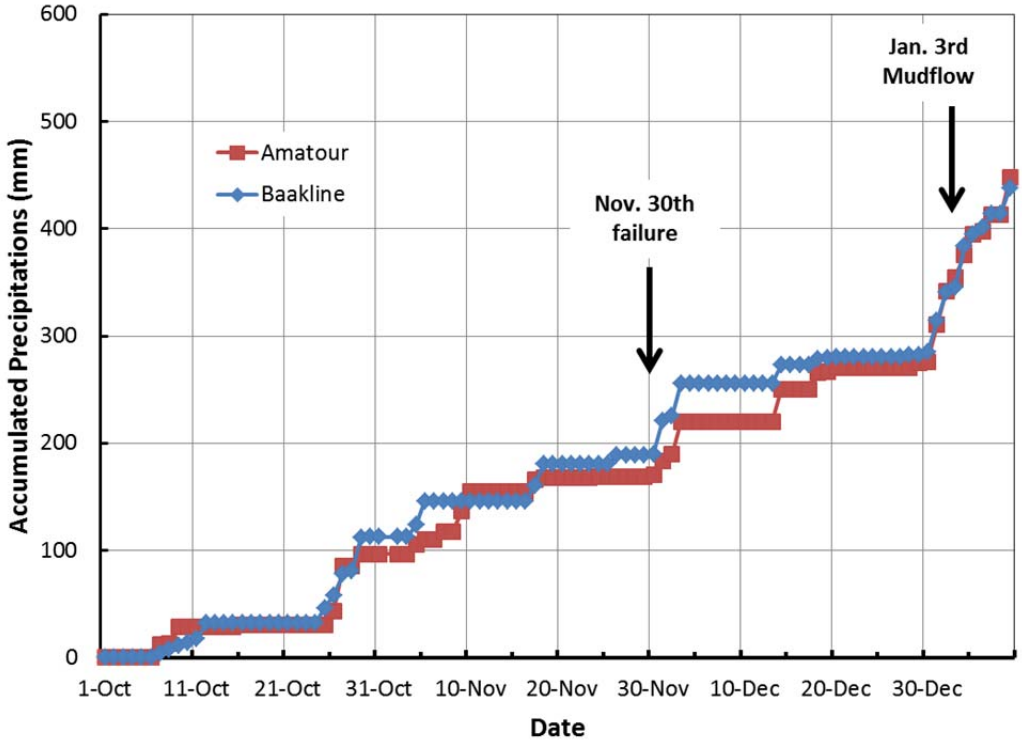

Figure 12: Rainfall data starting one month prior to the landslide

Failure Mechanism and Preliminary Evaluation of Current Conditions

- **Probable failure mechanism**

After collecting the feedback from local residents about the failure, watching the videos capturing the landslide that were shared on social media, and visiting the site, the GEER team developed the most probably failure mechanism shown in Figure 13 below.

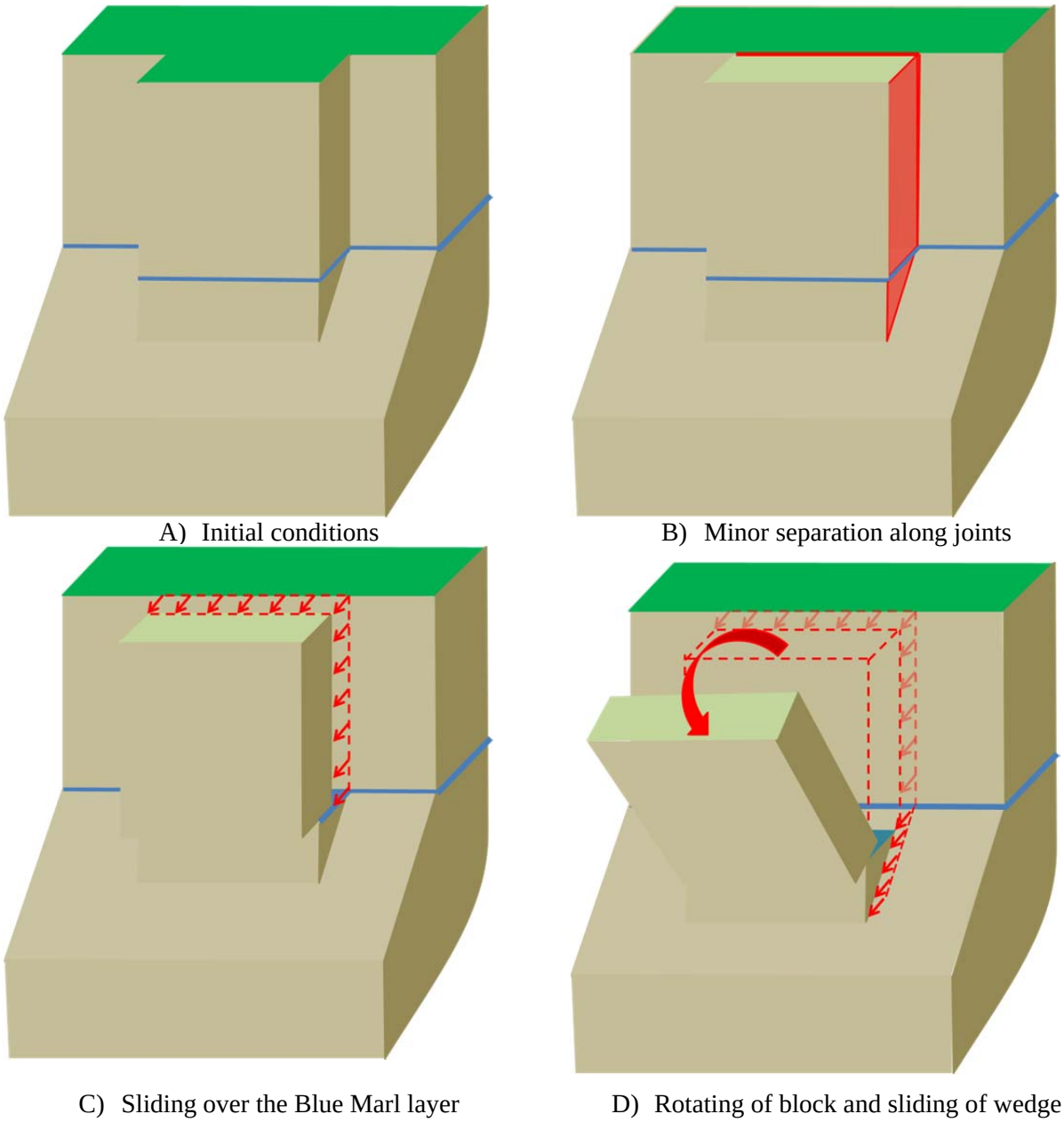

A) Initial conditions B) Minor separation along joints

C) Sliding over the Blue Marl layer D) Rotating of block and sliding of wedge

Figure 13: Proposed failure mechanism

Figure 13-A shows that a block of the rock mass, defined by the existing joints, represents the initial conditions. Figure 13-B shows the initial limited movement of the rock mass causing

separation between the block and surrounding rock. This behavior was evident during the site visit when looking at the cliff sides as can be seen in Figure 14. The surface crack shown in Appendix Figure A-4 is located on ground surface right above the vertical corner joint shown below. As a result of these cracks, water flow through the joints is cutoff and the grass on the surface exhibits a change in color from green to yellow. This can be seen by observing images taken from Google Earth at dates prior to the 2015 failure (Figure 15). Notice the change in the grass color.

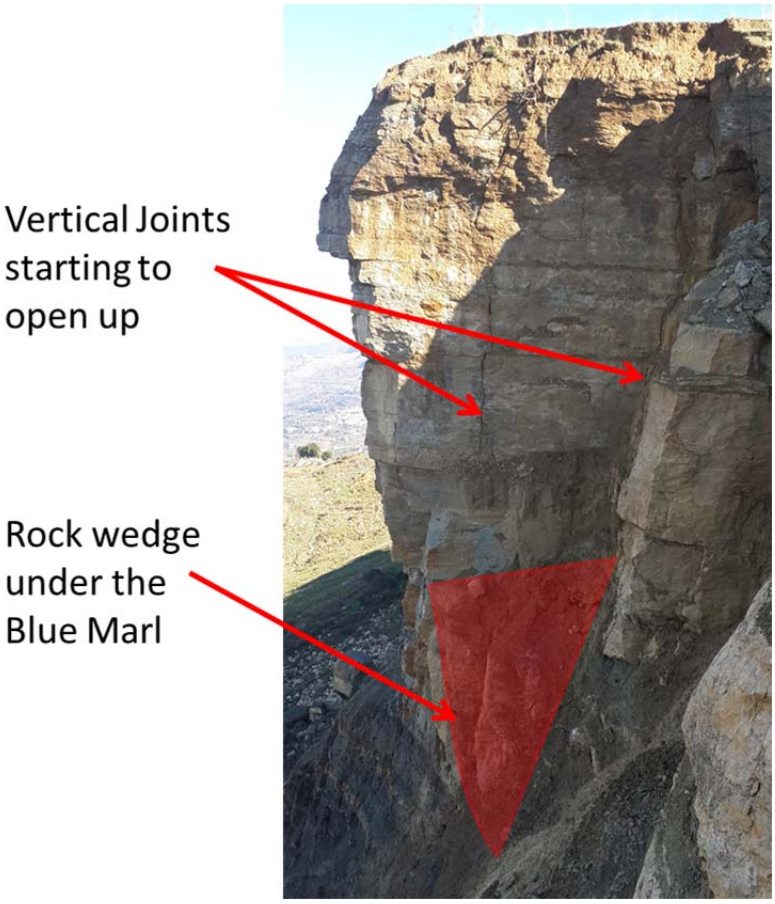

Figure 14: Side view of the cliff showing the highly jointed rock mass with some vertical joints stating to open up (Picture take at 33°42'00"N 35°37'38"E)

As the joints open, the water starts flowing down the joints (rather than across it) in addition to allowing more surface water to seep into the ground since the joint expansion is usually accompanied by cracks in the top soil extending to the surface. The water seeping through the vertical joints can now reach the Blue Marl layer (a high plasticity-low friction strata) causing its top portion to get saturated. The saturated Blue Marl, like all high plasticity clays, loses significant portion of its unsaturated strength once it gets saturated which creates a layer acting almost like a lubricant underneath the already mobilized rock mass, and thus facilitating its horizontal slippage (Figure 13-C). The horizontal slippage during the early stage of the rock mass failure can be seen during the video recordings (Figure 16). This theory can also help

explain local residents' observations of "blue rocks" shooting out of the cliffs. As the moving block separates from the cliff, it becomes solely supported on the weak Blue Marl layer, which could lead to bearing failures resulting in "squeezing" of the clay (the Blue Marl is constrained between top and bottom rock masses) and having parts of it pushed out of the face of cliff. This could have been mistakenly identified as small rocks shooting out of the cliffs.

Figure 15: Change in color of grass as joints open and cut water supply prior to failing in August 2014- Red line presents 2015 failure zone (pictures form Google Earth Pro)

Figure 16: Snapshot from video of landslide showing a lateral displacement of the rock mass with a gap created between it and the stable ground

As the block slides further, it starts creating a moment due to the overhanging portion of it resulting in rotational movement accompanied by failure in the edge of rock supporting the Blue Marl. The rotational movement after the initial sliding can be seen in the video referenced in the

earlier link starting at the 1:11 mark. This failure results in the wedge sliding down the slope after tensile cracks develop on along the backside. The rock wedge can be seen in the images of the site as shown in Figure 17.

Figure 17: Wedge previously supporting the Blue Marl (Picture generated form Point cloud 3D representation)

- **Volume of mobilized mass**

The pre-failure outline of the cliff was extracted from GoogleEarth's latest data (August 2014) and added to the DSM model created from the drone images. Coordinates of local fixtures (corner of buildings) were used to correct for any offset between the two. Figure 18 shows the resulting footprint of the failure area with an approximate cross-section of 700 m^2. The average thickness of the failed mass was estimated at 25 m and accounting for the angled back joint along which the rock block separated, the approximate volume of the failed material is estimated at 15,000 m^3 (165,000 yd^3).

Figure 18: Cross-sectional area of 2015 failure (Picture generated form Point cloud 3D representation)

- **Current conditions and risk of new failures (mapping high risk zones)**

Both landslides (2012 and 2015) occurred in the C3 formation. While the massive cliffs in the C3 formation appear to be of high quality rock, closer observation reveals a highly jointed rock mass (average joint spacing on the order of 1-2 m.) with dominant joints in the NorthWest – SouthEast and NorthEast – SouthWest directions at a rough spacing of 10m and 15m, respectively. The top soil has a low hydraulic conductivity and the C3 formation is classified as an unproductive basin due to its low hydraulic conductivity; however during site visits, it was observed that there were water springs at the top of the cliff that run year round. There was a small spring at the base of the cliff as well, all implying the presence of water flowing through the C3 formations joints. This water serves as the main source of natural irrigation for surface vegetation other than rain. Figure 15 shows the top of the cliffs covered with green vegetation in August 2014; since August is in the dry season in the area with limited rain, the green vegetation only source of water supply is the ground (only possible source of water in the ground is the joints). When a rock mass is mobilized along a set of joints, the opening of the joint increases and the joint start serving as a vertical drain rather than facilitating horizontal water flow. The reduced water supply to the vegetation on top of the unstable rock mass results in a change in its color (more yellowish green to light brown).

Using this information and studying the images of the area near the 2012 and 2015 landslides, the highest risk area was identified. Figure 19 shows a zone (below the dashed line)

that clearly marks a lighter shade of green vegetation compared to the vegetation further away from the cliff. This line falls on top of the extrapolated projection of the main NorthEast – SouthWest joint that generated the 2012 landslide. This high risk zone extends to the SouthWest corner of the house closest to the cliff and should be a major reason for concern for the overall stability of this house (which has been already evacuated).

Figure 19: High risk area based on vegetation color change, observed surface cracks and location of existing joints (Picture generated form Point cloud 3D representation)

References

- Dubertret, L., 1945, Carte Géologique de Jezzine 1/50000e Avec Notice Explicative. Beyrouth, République Libanaise, Ministère des Travaux Publics.
- Walley, C.D., 1983, A Revision of the Lower Cretaceous Stratigraphy of Lebanon. Geologische Rundschau, Stuttgart, Band 72, Heft 1, p. 377-388.
- Walley, C.D., 1997, The lithostratigraphy of Lebanon: a Review. Lebanese Scientific Bulletin, v. 10, p. 81-108.

Appendix

Figure A.1: local water spring at the top of the cliff, about 30m. from the face of the cliff and 20m. from the southeast corner of the 2012 failure.

Figure A.2: Highly jointed rock mass.

Figure A.3: Highly jointed rock mass.

Figure A.4: Surface cracks already well developed in the area between 2012 and 2015 failure.

Figure A.5: Surface water runoff at the base of the cliff

Figure A.6: Damage to backyard fence after 2015 landslide